Transitions in lithiumlike Cu^{26+} and berylliumlike Cu^{25+} of interest for x-ray laser research

C. M. Brown, J. O. Ekberg, U. Feldman, and J. F. Seely

E. O. Hulburt Center for Space Research, Naval Research Laboratory, Washington, D.C. 20375-5000

M. C. Richardson and F. J. Marshall

Laboratory for Laser Energetics, University of Rochester, Rochester, New York 14623-1299

W. E. Behring

Laboratory for Solar Physics and Astrophysics, Goddard Space Flight Center, Greenbelt, Maryland 20771

Received October 10, 1986; accepted December 23, 1986

Transitions in highly charged copper ions have been identified in the extreme-ultraviolet spectra from plasmas produced by the Omega laser at the University of Rochester. The 24 beams of the Omega laser were focused to separate spots of diameter 50 μm upon the surface of copper-coated targets 600 μm in diameter. The transitions in lithiumlike Cu^{26+} and berylliumlike Cu^{25+} of the type $n = 3$–4 were observed in the wavelength region 24 to 28 Å and were bright in the focal regions. The intensities of the Cu^{26+} $2p$–$3d$ and $3d$–$4f$ transitions indicate that a population inversion occurs between the $3d$ and $4f$ levels. Comparisons of the observed relative intensities of the Cu^{26+} transitions with calculated intensities indicate that the Cu^{26+} spectrum originates in a plasma region with an electron density of order of 10^{20} cm^{-3} and that collisional recombination is important for populating the $4f$ level. The $3d$–$4f$ transitions at 25.525 and 25.636 Å in Cu^{26+}, and the same transitions in neighboring elements, appear to be good candidates for achieving gain at wavelengths below the carbon absorption edge at 43.5 Å.

INTRODUCTION

Highly charged ions with one electron outside a closed shell are of interest for achieving population inversions and laser gain on transitions in the extreme-ultraviolet (XUV) and x-ray spectral regions. In a rapidly cooling plasma, the highly excited levels of these ions are populated by collisional recombination, and quasi-steady population inversions can occur during collisional and radiative cascade to lower levels. Such population inversions are a result of the rapid depopulation of the lower levels by radiative decay.

Population inversions in the Li I isoelectronic sequence have been observed in aluminum (atomic number $Z = 13$) and in a number of lower-Z elements.[1–4] Recently evidence for amplification at 105.7 and 127.9 Å was reported for aluminum and magnesium plasmas produced by line-focus laser irradiation.[5,6]

Coherent radiation in the XUV and x-ray wavelength regions is of particular interest for the study of organic materials. In order to obtain contrast through the absorption of the radiation in the specimen under study, it is advantageous to use radiation with a wavelength below the carbon absorption edge at 43.5 Å. The wavelength of the lasing transition decreases as the charge of the parent ion becomes larger, and in the Li I sequence one must use transitions in ions with $Z \geq 23$ to obtain wavelengths less than 43 Å.

In this paper we present the spectrum of highly charged copper ($Z = 29$) in the wavelength region from 8 to 220 Å. We have identified transitions of the type $n = 3$–4 in lithiumlike Cu^{26+} and in berylliumlike Cu^{25+} in the wavelength region 24 to 28 Å that have potential for achieving gain at wavelengths below the carbon absorption edge. The comparision of the observed intensities of the Cu^{26+} $2p$–$3d$ and $3d$–$4f$ transitions indicates that the $3d$ and $4f$ levels are inverted, and the ratio of the reduced populations is approximately $4f/3d = 3$. Based on a numerical simulation of the Cu^{26+} spectrum, we find that the Cu^{26+} transitions originate in a plasma region with electron density of the order of 10^{20} cm^{-3} and that collisional recombination contributes substantially to the population of the $4f$ level.

EXPERIMENT

The spectra were recorded at the University of Rochester's Laboratory for Laser Energetics. The radiation was emitted by plasmas produced by using the Omega laser to heat copper targets to high temperatures. Targets were solid plastic spheres 600 μm in diameter coated with 1 μm of copper. All 24 beams of the Omega laser were focused onto the target surface in a spherically symmetric pattern of spots, as shown in Fig. 1(a). The diameter of each focal spot was 50 μm. The wavelength of the laser irradiation was 351 nm, the energy in each beam was 50 J, and the pulse duration was 450 psec.[7,8] The average intensity of laser irradiation in each focal spot was 6×10^{15} W/cm^2.

Spectra were recorded by a 3-m grazing-incidence spectrograph.[9] The spectrum from 8 to 60 Å was recorded using a

0740-3224/87/040533-06$02.00

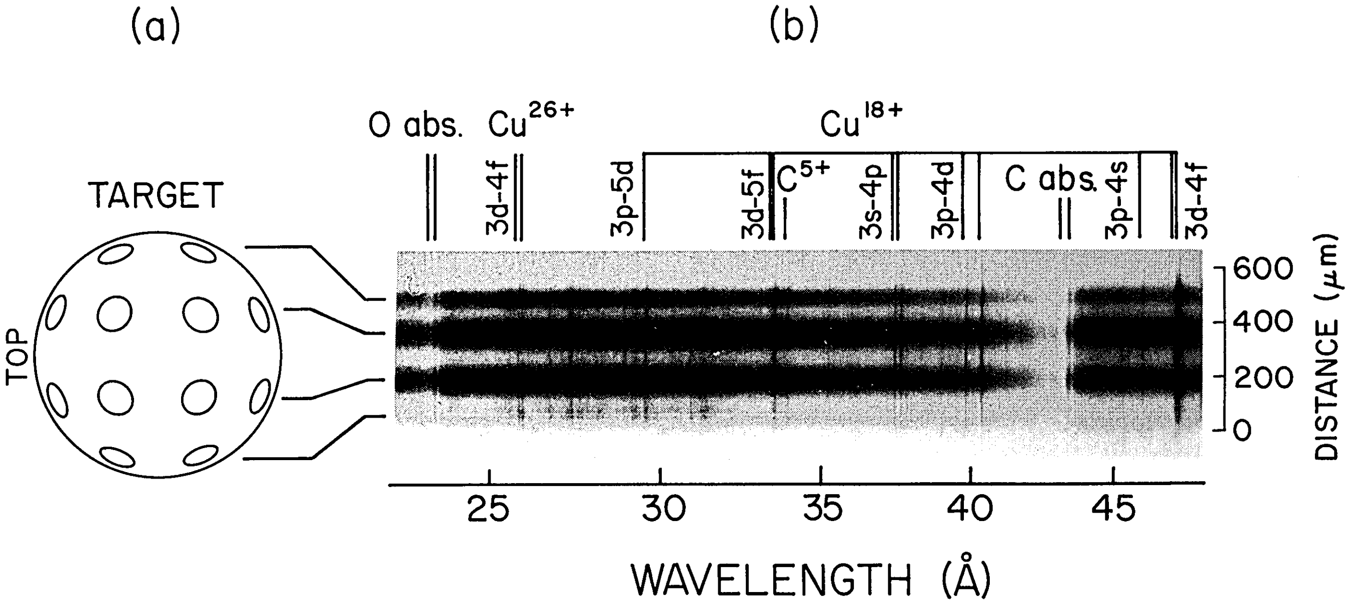

Fig. 1. (a) The pattern of laser focal spots on the hemisphere of the target facing the spectrograph. The diameter of each focal spot is 50 μm, and the diameter of the copper-coated target is 600 μm. (b) The spectrum from 22 to 48 Å showing the $3d$–$4f$ transitions in lithiumlike Cu^{26+} near 25.6 Å, the $n = 3$–4 and $n = 3$–5 transitions in sodiumlike Cu^{18+}, and the C^{5+} Lyman-α transition at 33.736 Å. The carbon and oxygen inner-shell absorption features are present at 43.5 and 23.3 Å, respectively. The distance across the target is indicated by the scale at the right-hand side of the spectrum.

grating blazed at 2° 35′, and the spectrum from 20 to 300 Å was recorded using a grating blazed at 4° 7′. Each grating was gold coated and had 1200 lines/mm, and the angle of incidence was 88°. Spectra were recorded on Kodak Type SWR plates, and the radiation from five laser shots was integrated into each exposure.

Radiation from the target was focused onto the entrance slit of the spectrograph by a cylindrical mirror that was positioned 130 cm from the target and 70 cm in front of the entrance slit. The line image formed by the mirror was crossed at an angle of 1° with the entrance slit, and this provided spatial resolution of the target in one dimension. This imaging system is described in detail in Ref. 10.

Part of a typical spectrum is shown in Fig. 1(b). Since the spectrum from the target is spatially resolved in one dimension, four bright bands of continuum appear on the plate that originate in the four rows of focal spots. Between these bands, three gaps in the spectrum occur that originate in the regions of the target between the rows of focal spots. The spectral lines from the highly charged copper ions (such as Cu^{26+}) are much brighter in the band regions than in the gap regions, and the spectral lines from the lower ionization stages (such as Cu^{18+}) are bright in the gap regions. The C^{5+} Lyman-α transition at 33.736 Å is intense in the band regions, and this indicates that the 1-μm copper coating was penetrated in the focal spots and the underlying plastic sphere was heated by the laser irradiation. The burnthrough of the 1-μm copper coating is consistent with that described in previous work.[11] Also indicated in Fig. 1(b) are inner-shell absorption features of carbon and oxygen at 43.5 and 23.3 Å, respectively. This absorption takes place in contaminants on the mirror surface and to a lesser extent on the grating surface. The absorption features diminished substantially when the mirror was subsequently coated with gold.

SPECTRAL LINE IDENTIFICATIONS

Transitions in sodiumlike and neodymiumlike copper were identified in the spectra. The wavelengths of these transitions were measured previously,[12–18] and we used these previous measurements to establish a wavelength scale in the present work. The estimated accuracy of this wavelength scale is ±0.010 Å for lines longer than 12 Å and ±0.005 Å for shorter-wavelength lines. The separation between nearby lines can be measured to an accuracy of ±0.003 Å. Transitions in $Cu^{20+-23+}$ were also identified. These transitions were reported in Refs. 19 and 20.

Our identification of the transitions in Cu^{26+} was based on the appearance of the spectral lines on the plate and on the calculated wavelengths and intensities. The measured wavelengths and the classification of the spectral lines in Cu^{26+} are presented in Table 1. Measured wavelengths are in excellent agreement with the calculations of Vainshtein and Safronova.[21] The Cu^{26+} energy levels derived from our measured wavelengths are listed in Table 2. The ionization limit was determined by using the core polarization expressions of Edlén,[23] and the results are presented in Table 3. The adopted ionization limit for Cu^{26+} is $(20\,870 \pm 3) \times 10^3$ cm^{-1}.

The measured wavelengths and the classification of spectral lines in Cu^{25+} are listed in Table 4. The identification of these transitions was based on wavelengths and line strengths calculated by using Cowan's computer program.[24] Many of the $n = 2$–3 transitions were observed by Boiko *et al.*,[16,17] and those observations are also presented in Table 4. Although jj coupling is perhaps more appropriate than LS coupling for $Z = 29$, we have retained the LS coupling level designations for consistency with earlier work. In some cases, our designations differ from those of Refs. 16 and 17. Transitions between 6 and 9 Å in Cu^{26+} and Cu^{25+} were also

Table 1. Wavelengths (in angstroms) and Classification of Spectral Lines for Cu^{26+}

Transition	Int.[a]	Meas.	Calc.[b]	Calculated Intensity[c] 10^{19}	10^{20}	10^{21}
$2s\ ^2S_{1/2}$–$2p\ ^2P_{3/2}$	4	153.504	153.563	35	4.9	0.5
$2s\ ^2S_{1/2}$–$2p\ ^2P_{1/2}$	–	224.9[d]	225.024	76	0.6	0.1
$2s\ ^2S_{1/2}$–$3p\ ^2P_{3/2}$	20	8.401[e]	8.404	10.2	7.5	7.2
$2s\ ^2S_{1/2}$–$3p\ ^2P_{1/2}$	10	8.445[e]	8.448	7.7	5.3	4.6
$2p\ ^2P_{1/2}$–$3d\ ^2D_{3/2}$	15	8.691[e]	8.695	20.4	15.7	14.3
$2p\ ^2P_{3/2}$–$3d\ ^2D_{5/2}$	25	8.837[e]	8.839	25.0	25.0	25.0
$2p\ ^2P_{3/2}$–$3d\ ^2D_{3/2}$	2	8.856[e]	8.854	3.9	3.0	2.7
$2p\ ^2P_{1/2}$–$3s\ ^2S_{1/2}$	2	8.876[f]	8.873	2.7	1.3	0.8
$2p\ ^2P_{3/2}$–$3s\ ^2S_{1/2}$	10	9.042[f]	9.039	5.7	2.8	1.7
$3s\ ^2S_{1/2}$–$4p\ ^2P_{3/2}$	1	24.291	24.302	0.2	0.2	0.1
$3p\ ^2P_{1/2}$–$4d\ ^2D_{3/2}$	1	24.943	24.930	0.2	0.1	0.1
$3p\ ^2P_{3/2}$–$4d\ ^2D_{5/2}$	3	25.291[g]	25.264	0.2	0.2	0.3
$3d\ ^2D_{3/2}$–$4f\ ^2F_{5/2}$	6	25.543[g]	25.559[h]	0.2	0.2	0.3
$3d\ ^2D_{5/2}$–$4f\ ^2F_{7/2}$	7	25.646	25.660[h]	0.2	0.2	0.4
$3d\ ^2D_{5/2}$–$4p\ ^2P_{3/2}$	1	25.893	25.876	0.02	0.02	0.02

[a] Intensities based on visual estimates of plate darkening.
[b] Calculated wavelengths of Vainshtein and Safronova.[21]
[c] Intensities calculated using Klapisch's computer package for the indicated electron densities (in cm^{-3}). The intensities are normalized by setting the intensity of the $2p\ ^2P_{3/2}$–$3d\ ^2D_{5/2}$ transition equal to 25.
[d] Predicted wavelength based on the measured wavelengths of other transitions.
[e] Transitions also observed by Burkhalter *et al.*[22] with a crystal spectrometer during the same laser shots.
[f] Blended with Cu^{25+} transitions.
[g] Possibly effected by Cu^{18+} transitions.[18]
[h] Calculated using the polarization expressions of Edlén.[23]

observed simultaneously by Burkhalter *et al.*,[22] who used a flat crystal spectrometer during the same laser shots.

TRANSITION INTENSITIES

The intensities of the Cu^{26+} transitions were calculated by using the collisional-radiative computer program of M. Klapisch. This calculation included collisional excitation and deexcitation and radiative decay but not recombination processes and opacity effects. The intensities calculated for an electron temperature of 1 keV and for several electron densities between 10^{19} and 10^{21} cm^{-3} are listed in Table 1. We have normalized our calculated intensities to that of the $2p\ ^2P_{3/2}$–$3d\ ^2D_{5/2}$ transition.

Boiko *et al.*[25] calculated the intensities of the three Cu^{26+} transitions $2s\ ^2S_{1/2}$–$3p\ ^2P_{3/2}$, $2p\ ^2P_{3/2}$–$3s\ ^2S_{1/2}$, and $2p\ ^2P_{1/2}$–$3d\ ^2D_{3/2}$ relative to the intensity of the transition $2p\ ^2P_{3/2}$–$3d\ ^2D_{5/2}$. These three intensity ratios are in good agreement with our calculated results. The calculated intensity ratios were practically independent of electron temperature over the range of 0.5 to 1.1 keV.[25]

In an optically thin plasma, the intensities of the Cu^{26+} spectral lines are proportional to the populations in the upper levels of the transitions. At low electron densities ($\leq 10^{18}$ cm^{-3}), these excited levels are populated primarily by electron collisional excitation from lower levels and are depopulated by radiative decay. The $2p$ level is populated primarily by collisional excitation from the $2s$ ground level. As the electron density increases, the intensities of the $2s$–$2p$ transitions increase linearly with electron density until collisional deexcitation of the $2p$ level begins to compete with radiative decay. At still higher densities, the population of

Table 3. Ionization Energies (in 10^3 cm^{-1}) for Cu^{26+}

Level	J	Δ_p[a]	T_H[b]	E[c]	E_i[d]
$3d$	3/2	2.1	8917.4	11951	20 871
	5/2	2.1	8898.2	11968	20 868
$4d$	3/2	1.2	5015.0	15850	20 866
	5/2	1.2	5006.9	15857	20 865
$4f$	5/2	0.04	5006.9	15866	20 873
	7/2	0.04	5002.9	15867	20 870

[a] Core polarization energy from Edlén.[23]
[b] Calculated relativistic hydrogenic energy.
[c] Experimentally determined excitation energy.
[d] Ionization energy $E_i = \Delta_p + T_H + E$. The adopted ionization energy is $(20\,870 \pm 3) \times 10^3$ cm^{-1}.

Table 2. Observed Level Values (in 10^3 cm^{-1}) for Cu^{26+}

Term	J	Meas. Energy	Interval	n^*	Δn^*	Calc. Energy[a]	Interval
$2s\ ^2S$	1/2	0		1.9578		0	
$2p\ ^2P$	1/2	444.40[a]		1.9790		444.40	
			207.1		0.0101		206.80
	3/2	651.45 ± 0.2		1.9891		651.20	
$3s\ ^2S$	1/2	11 711 ± 10		2.9554		11 714	
$3p\ ^2P$	1/2	11 841 ± 10		2.9766		11 837	
			62 ± 5		0.0103		62
	3/2	11 903 ± 10		2.9869		11 899	
$3d\ ^2D$	3/2	11 951 ± 10		2.9949		11945	
			17 ± 5		0.0029		19
	5/2	11 968 ± 10		2.9977		11 964	
$4p\ ^2P$	3/2	15 829 ± 15		3.9836		15 829	
$4d\ ^2D$	3/2	15 850 ± 15		3.9920		15 849	
			7 ± 5		0.0028		8
	5/2	15 857 ± 15		3.9948		15 857	
4f ^2F	5/2	15 866 ± 15		3.9983			
			1 ± 5		0.0004		
	7/2	15 867 ± 15		3.9987			

[a] Calculated levels from Vainshtein and Safronova.[21]

Table 4. Wavelengths (in angstroms) and Classification of Spectral Lines for Cu^{25+}

Transition	Present Work			Previous Work	
	Int.[a]	Meas.	Calc.[b]	Meas.[c]	Calc.[d]
$2s2p\ ^3P_2$–$2p3p\ ^1D_2$	3	8.551	8.545	8.551	8.544
$2s2p\ ^3P_2$–$2p3p\ ^3P_2$	12	8.618	8.611	8.653	8.650
$2s^2\ ^1S_0$–$2s3p\ ^1P_1$			8.654		8.663
	3	8.661			
$2s^2\ ^1S_0$–$2s3p\ ^3P_1$			8.694		8.705
$2s2p\ ^1P_1$–$2p3p\ ^1D_2$	5	8.773	8.780	8.772	8.766
$2s2p\ ^3P_0$–$2s3d\ ^3D_1$	2	8.876[e]	8.874		8.899
$2s2p\ ^3P_1$–$2s3d\ ^3D_2$			8.906	8.933	8.929
	5	8.908			
$2s2p\ ^3P_1$–$2s3d\ ^3D_1$			8.912		8.934
$2p^2\ ^3P_2$–$2p3d\ ^1F_3$			8.962	8.981[g]	8.973
$2p^2\ ^3P_1$–$2p3d\ ^3P_1$	8	8.970[f]	8.969		8.994
$2s2p\ ^1P_1$–$2p3p\ ^1P_1$			8.990	8.981[g]	8.984
$2p^2\ ^3P_0$–$2p3d\ ^3D_1$			9.020		9.043
$2s2p\ ^3P_2$–$2s3d\ ^3D_3$	20	9.026[f]	9.022		9.041
$2s2p\ ^3P_2$–$2s3d\ ^3D_2$			9.032		9.051
$2p^2\ ^3P_2$–$2p3d\ ^3D_3$	10	9.042[e,f]	9.038		9.053
$2p^2\ ^1D_2$–$2p3d\ ^1F_3$	10	9.131[f]	9.124		9.131
$2p^2\ ^3P_1$–$2p3d\ ^3D_2$	3	9.149	9.139		9.155
$2p^2\ ^1D_2$–$2p3d\ ^3D_2$			9.182		
$2s2p\ ^3P_1$–$2s3s\ ^3S_1$			9.197		9.225
	12	9.194[f]			
$2p^2\ ^3P_2$–$2p3d\ ^3F_3$			9.201		
$2s2p\ ^1P_1$–$2s3d\ ^1D_2$			9.223	9.233	9.227
$2p^2\ ^1S_0$–$2p3d\ ^1P_1$	6	9.324	9.317	9.331	9.336
$2s2p\ ^3P_2$–$2s3s\ ^3S_1$	15	9.359	9.331	9.355	9.355
$2p^2\ ^1D_2$–$2p3d\ ^3P_2$	3	9.375	9.362	9.373	9.368
$2p^2\ ^3P_1$–$2p3s\ ^3P_0$			9.447	9.520	9.524
$2p^2\ ^1D_2$–$2p3s\ ^1P_1$			9.451		9.523
$2s2p\ ^1P_1$–$2s3s\ ^1S_0$	1	9.489	9.539		
$2p^2\ ^1S_0$–$2p3s\ ^1P_1$	3	9.746	9.671	9.737	9.746
$2p3d\ ^3F_4$–$2p4f\ ^3G_5$	1	27.013	26.939		
$2s3d\ ^3D_3$–$2s4f\ ^3F_4$	1	27.182	27.084		
$2p3d\ ^3F_3$–$2p4f\ ^3G_4$	1	27.395	27.296		
$2s^2\ ^1S_0$–$2s2p\ ^1P_1$	10	111.071[h]	109.97		111.117[i]

[a] Intensity based on visual estimate of plate darkening.
[b] Calculation using Cowan's computer program.[24]
[c] Measured wavelengths and line identifications of Boiko *et al.*[16,17]
[d] Calculated wavelengths of Safronova.[16,17]
[e] Blended with Cu^{26+} transitions.
[f] Transitions also observed by Burkhalter *et al.*[22] with a crystal spectrometer during the same laser shots.
[g] Multiply classified line.
[h] Blended with Cu^{22+} transition.
[i] Calculation of Edlén.[29]

the $2p$ level reaches a plateau value where collisional excitation is balanced by collisional deexcitation. In this collisionally saturated regime, the intensities of the $2s$–$2p$ transitions are nearly independent of electron density in optically thin plasmas.

If the abundance of the Cu^{26+} ionization stage is high and if the transverse size of the plasma is large, then reabsorption of the $2s$–$2p$ radiation by the $2s$ ground state may be significant. In this case, the intensities of the $2s$–$2p$ transitions may actually decrease with increasing electron density. For the present plasma with a radius in the transverse direction of 25 μm, the optical depths of all the transitions under consideration are less than unity, and reabsorption of the ground-state radiation is negligible.

The $3d$ level is populated primarily by collisional excitation from the $2p$ level. As the population of the $2p$ level increases with electron density, the intensity of the $2p$–$3d$ transition also increases until the collisional deexcitation of the $3d$ level competes with radiative decay. Owing to the larger excitation energy of the $3d$ level, the collisional saturation of the $3d$ level occurs at a higher density than does the saturation of the $2p$ level. As is shown in Table 1, at low electron densities the calculated $2s$–$2p$ intensities are larger than the $2p$–$3d$ intensities. At densities of 10^{20} cm^{-3} and greater, the $2s$–$2p$ transitions are collisionally saturated, and the $2p$–3d transitions have the higher intensities. Since the experimentally observed $2s\ ^2S_{1/2}$–$2p\ ^2P_{3/2}$ transition was very weak and the $2s\ ^2S_{1/2}$–$2p\ ^2P_{1/2}$ transition was not observed at all, these transitions must have originated in a plasma region with an electron density of the order of 10^{20} cm^{-3}.

The $4f$ level cannot be efficiently populated directly from the $n = 2$ levels, and the excitation rate of the $4f$ level from the $3d$ level is small owing to the low $3d$ population. The calculated intensities of the $3d$–$4f$ transitions are much lower than the observed intensities, and this indicates that the

$4f$ level is populated primarily by recombination processes that are not included in the model. As a result of the small radius of the focal spots (25 μm) and the short duration of the heating pulse (450 psec), it is likely that the plasma rapidly cools by expansion and by radiation and that recombination is a more important mechanism than collisional excitation for the population of the $4f$ level.

The absence in the observed spectra of transitions from the levels with $n \geq 5$ is the result of the collisional mixing of these levels with the continuum. At an electron density of 3×10^{21} cm^{-3}, the collision limit[26] occurs at $n = 5$, and this implies that the levels with $n \geq 5$ are likely to be collisionally depopulated.

POPULATION INVERSION

The ratio of the populations of two levels can be determined from the ratio of the intensities of the transitions from the two levels. The intensity of an optically thin transition is

$$I = ANhc/\lambda, \quad (1)$$

where A is the spontaneous decay rate and N is the population of the upper level. The ratio of the reduced populations (populations divided by statistical weights) of two levels is

$$(N_2/g_2)/(N_1/g_1) = (I_2/I_1)(\lambda_2/\lambda_1)(g_1A_1/g_2A_2), \quad (2)$$

where g is the statistical weight. If level 2 has a higher excitation energy than level 1 and $N_2/g_2 > N_1/g_1$, then the populations of the two levels are said to be inverted. In this case, the radiation from the transition $2 \rightarrow 1$ can be amplified in a linear plasma.

In order to look for population inversions by using the above method, one must measure the relative intensities of two spectral lines. The wavelengths of the Cu^{26+} $n = 2$–3 and $n = 3$–4 transitions of interest are approximately 9 and 25 Å, respectively, and it is difficult in the present experiment to determine the sensitivity of the spectrograph at these two wavelengths. However, an approximate calibration can be performed that is based on the intensity of the continuum radiation as a function of wavelength. This continuum radiation results from radiative recombination and from free–free scattering. For an electron temperature of 1 keV, the continuum near 10 Å is due primarily to radiative recombination, and this calculated continuum is nearly independent of wavelength for the present plasma conditions.[27] The observed continuum changes by less than a factor of 2 between 9 and 25 Å, and this implies that the observed intensities of the Cu^{26+} $n = 2$–3 and $n = 3$–4 transitions that are listed in Table 1 are accurate to approximately a factor of 2.

Using the observed intensities and the calculated A values of the Cu^{26+} $2p$–$3d$ and $3d$–$4f$ transitions, we obtain from Eq. (2) a reduced population ratio of approximately $4f/3d = 3$. We believe that this value is accurate to a factor of 2. It appears that the $3d$ and $4f$ levels were inverted in the experiment, and the likely inversion mechanism is collisional recombination and cascading. The observed intensities of the $2s$–$3p$ and $3p$–$4d$ transitions indicate that the populations of the $3p$ and $4d$ levels were not inverted.

DISCUSSION

Based on the observed intensities of the Cu^{26+} $2p$–$3d$ and $3d$–$4f$ transitions, the $3d$ and $4f$ levels appear to be inverted in the present experiment. The accuracy of this determination could be improved by a branching-ratio calibration of the sensitivity of the spectrograph based on the intensities of the $2p$–$4d$ transitions at 6.5 Å and the $3p$–$4d$ transitions at 25 Å. However, it is difficult to observe 6.5-Å lines with a grating. In order to perform this branching-ratio calibration, one must use ions with atomic numbers $Z \leq 26$ and $2p$–$4d$ wavelengths greater than 8 Å. Then the $2p$–$4d$ and $3p$–$4d$ transitions can be observed simultaneously, and the branching-ratio calibration will result in a more accurate measurement of the $2p$–$3d$ and $3d$–$4f$ intensities of the $4f/3d$ population inversion.

The computational modeling can be improved by the addition of recombination into highly charged levels and the inclusion of the time dependence of the transient plasma. Such modeling of the Cu^{26+} plasma is in progress.[28] We also note that the population inversion is determined from time-integrated data, and the instantaneous population inversion may be higher.

ACKNOWLEDGMENTS

Calculations of the intensities of the Cu^{26+} transitions were done at Lawrence Livermore National Laboratory using M. Klapisch's computer program. We thank W. Goldstein and C. Cerjan for assistance in performing these calculations. We also thank A. Sureau for comments on the manuscript and for communicating computational results. W. Watson and the Omega Laser Operations Staff provided expert technical assistance. This research was supported by the U.S. Department of Energy under contract DE-AI08-84-DP40092/26. The research and materials incorporated in this work were partially developed at the National Laser Users Facility at the University of Rochester's Laboratory for Laser Energetics, with financial support from the U.S. Department of Energy under contract DE-AC08-80DP40124.

J. O. Ekberg is also with Sachs/Freeman Associates, Landover, Maryland 20785; permanent address, Department of Physics, University of Lund, Lund, Sweden.

REFERENCES

1. E. Ya. Kononov, K. N. Koshelev, Yu. A. Levykin, Yu. V. Sidelnikov, and S. S. Churilov, "Population inversion of Al XI in a laser plasma," Sov. J. Quantum Electron. **6**, 308 (1976).
2. P. Jaegle, G. Jamelot, A. Carillon, A. Klisnick, A. Sureau, and H. Guennou, "Amplification of spontaneous emission in aluminum and magnesium plasmas," in *Laser Techniques in the Extreme Ultraviolet*, S. E. Harris and T. B. Lucatorto, eds., AIP Conf. Proc. **119**, 468 (1984).
3. S. Suckewer, C. H. Skinner, D. R. Voorhees, H. M. Milchberg, C. Keane, and A. Semet, "Population inversion and gain measurements for soft x-ray laser development in a magnetically confined plasma column," IEEE J. Quantum Electron. **19**, 1855 (1983).
4. S. Suckewer, C. Keane, H. Milchberg, C. H. Skinner, and D. Voorhees, "Recent experiments on soft x-ray laser development in a confined plasma column," in *Laser Techniques in the Extreme Ultraviolet*, S. E. Harris and T. B. Lucatorto, eds., AIP Conf. Proc. **119**, 55 (1984).
5. G. Jamelot, A. Klisnick, A. Carillon, H. Guennou, A. Sureau, and P. Jaegle, "Amplification of soft x-ray spontaneous emission in aluminum and magnesium plasmas," J. Phys. B **18**, 4647 (1985).
6. P. Jaegle, A. Carillon, A. Klisnick, G. Jamelot, H. Guennou, and A. Sureau, "Soft x-ray amplification in recombining aluminum plasma," Europhys. Lett. **1**, 555 (1986).

7. J. M. Soures, R. J. Hutchison, S. D. Jacobs, L. D. Lund, R. L. McCrory, and M. C. Richardson, "Omega: A short wavelength laser for fusion experiments," in *Proceedings of the Tenth Symposium on Fusion Engineering* (Institute of Electrical and Electronic Engineers, New York, 1984), p. 1392.
8. M. C. Richardson, P. W. McKenty, F. J. Marshall, C. P. Verdon, J. M. Soures, R. L. McCrory, O. Barnouin, R. S. Craxton, J. Delettrêz, R. L. Hutchison, P. A. Jaanimagi, R. Keck, T. Kessler, H. Kim, S. A. Letzring, D. M. Roback, W. Seka, S. Skupsky, B. Yaakobi, S. M. Lane, and S. Prussin, "Ablatively driven targets imploded with the 24 UV beam Omega system," in *Proceedings of the 7th Meeting on Laser Interaction and Related Plasma Phenomena*, Hora, H. ed. (Plenum, New York, 1986), Vol. 7.
9. W. E. Behring, R. J. Ugiansky, and U. Feldman, "High resolution rocket EUV solar spectrograph," Appl. Opt. **12**, 528 (1973).
10. W. E. Behring, C. M. Brown, U. Feldman, J. F. Seely, J. H. Underwood, M. C. Richardson, and F. J. Marshall, "Grazing incidence technique to obtain spatially resolved spectra from laser heated plasmas," submitted to Appl. Opt.
11. B. Yaakobi, O. Barnouin, J. Delettrez, L. M. Goldman, R. Marjoribanks, R. L. McCory, M. C. Richardson, and J. M. Soures, "Thermal transport measurements in six-beam, ultraviolet irradiation of spherical targets," J. Appl. Phys. **57**, 4354 (1985).
12. U. Feldman, L. Katz, W. E. Behring, and L. Cohen, "Spectra of Fe, Co, Ni, and Cu isoelectronic with Na I and Mg I," J. Opt. Soc. Am. **61**, 91 (1971).
13. E. Ya. Kononov, A. N. Ryabtsev, and S. S. Churilov, "Spectra of sodium-like ions Cu XIX–Br XXV," Phys. Scr. **19**, 328 (1979).
14. J. Sugar and V. Kaufman, "Copper spectra in a laser-generated plasma: measurements and classifications of Cu XII to Cu XXI," J. Opt. Soc. Am. B **3**, 704 (1986).
15. H. Gordon, M. G. Hobby, and N. J. Peacock, "Classification of the x-ray spectra of transitions in the Ne, F, and O I isoelectronic sequences of the elements from iron to bromine and in the Na I isoelectronic sequence of gallium to bromine," J. Phys. B **13**, 1985 (1980).
16. V. A. Boiko, A. Ya. Faenov, and S. A. Pikuz, "X-ray spectroscopy of multiply charged ions from laser plasmas," J. Quant. Spectrosc. Rad. Trans. **19**, 11 (1978).
17. V. A. Boiko, S. A. Pikuz, U. I. Safronova, and A. Ya. Faenov, "Spectra of Be-like ions with nuclear charge $Z = 22, \ldots, 34$ from laser-produced plasmas," J. Phys. B **10**, 1253 (1977).
18. B. Edlén, "The transitions $3s$–$3p$ and $3p$–$3d$, and the ionization energy in the Na I isoelectronic sequence," Phys. Scr. **17**, 565 (1978).
19. E. Ya. Kononov, V. I. Kovalev, A. N. Ryabtsev, and S. S. Churilov, "Laser-plasma spectra of ions of elements from Fe to Br with 15–24 lost electrons, recorded in the 50–150 Å range," Sov. J. Quantum Electron. **7**, 111 (1977).
20. W. E. Behring, J. F. Seely, S. Goldsmith, L. Cohen, M. Richardson, and U. Feldman, "Transitions of the type $2s$–$2p$ in highly ionized Cu, Zn, Ga, and Ge," J. Opt. Soc. Am. B **2**, 886 (1985).
21. L. A. Vainshtein and U. I. Safronova, "Energy levels of He- and Li-like ions (states $1snl$, $1s^2nl$ with $n = 2$–5)," Phys. Scr. **31**, 519 (1985).
22. P. G. Burkhalter, D. A. Newman, and D. Rosen, Naval Research Laboratory, Washington, D.C. 20375 (personal communication, 1986).
23. B. Edlén, "Accurate semi-empirical formulae for the energy structure of Li-like spectra," Phys. Scr. **19**, 255 (1979).
24. R. D. Cowan, Los Alamos National Laboratory, Los Alamos, N.M. 87545 (personal communication, 1985).
25. V. A. Boiko, B. A. Brunetkin, A. Ya. Faenov, S. Ya. Hahalin, I. Yu. Skobelev, and K. A. Shilov, "Spectra of multiply-charged lithium-like ions in a high-temperature plasma," Phys. Scr. **30**, 59 (1984).
26. H. R. Griem, *Plasma Spectroscopy* (McGraw-Hill, New York, 1964).
27. T. F. Stratton, "X-ray spectroscopy," in *Plasma Diagnostic Techniques*, R. H. Huddlestone and S. L. Leonard, eds. (Academic, New York, 1965), p. 388.
28. A. Sureau, H. Guennou, and C. Moller, Université de Paris-Sud, 91405 Orsay, France (personal communication, 1986).
29. B. Edlén, "Comparison of theoretical and experimental level values of the $n = 2$ complex in ions isoelectronic with Li, Be, O, and F," Phys. Scr. **28**, 51 (1983).